





Article

Prediction of Vehicle Crashworthiness Parameters using Piecewise Lumped Parameters and Finite Element Models

Bernard B. Munyazikwiye^{1,2*} , Dmitry Vysochinskiy¹ , Mikhail Khadyko³  and Kjell G. Robbersmyr¹ 

¹ Department of Engineering Sciences, University of Agder, Jon Lilletuns Vei 9, 4879, Grimstad, Norway; bernard.munyazikwiye@uia.no, kjell.g.robbersmyr@uia.no, dmitry.vysochinskiy@uia.no

² Department of Mechanical and Energy Engineering, College of Science and Technology, University of Rwanda, Avenue de l'Armée, PoBox 3900, Kigali, Rwanda; bmunyazikwiye@ur.ac.rw

³ Department of Structural Engineering, Norwegian University of Science and Technology, Richard Birkelands Vei 1A, 7491, Trondheim, Norway; mikhael.khadyko@ntnu.no

* Correspondence: bernard.munyazikwiye@uia.no, bmunyazikwiye@ur.ac.rw; Tel.: +250 788 842 534

Version September 3, 2018 submitted to Preprints

Abstract: Estimating the vehicle crashworthiness parameters experimentally is expensive and time consuming. For these reasons different modelling approaches are utilized to predict the vehicle behaviour and reduce the need for full-scale crash testing. The earlier numerical methods used for vehicle crashworthiness analysis were based on the use of lumped parameters models (LPM), a combination of masses and nonlinear springs interconnected in various configurations. Nowadays, the explicit nonlinear finite element analysis (FEA) is probably the most widely recognized modelling technique. Although informative, finite element models (FEM) of vehicle crash are expensive both in terms of man-hours put into assembling the model and related computational costs. A simpler analytical tool for early analysis of vehicle crashworthiness could greatly assist the modelling and save time. In this paper a simple piecewise LPM composed of a mass-spring-damper system, is used to estimate the vehicle crashworthiness parameters, focusing on the dynamic crush and the acceleration severity index (ASI). The model is first calibrated against a full-scale crash test and a FEM, post-processed with the LS-DYNA software, at an impact velocity of 56 km/h. The genetic algorithm is used to calibrate the model by estimating the piecewise lumped parameters (stiffness and damping of the front structure of the vehicle). After calibration, the LPM is applied to a range of velocities (40, 48, 64 and 72 km/h). The predictions for crashworthiness parameters from the LPM were compared with the predictions from the FEA and the results are much similar. It is shown that the LPM can assist in crash analysis, since LPM has some predictive capabilities and requires less computation time in comparison with the explicit nonlinear FEA.

Keywords: Piecewise Lumped Parameters; Finite Element Analysis; Dynamic Crush; Acceleration Severity Index

1. Introduction

Car accidents are among the major causes of mortality in modern society. In automotive industry, safety is one of the design considerations. Usually, full-scale crash tests (FSCT) are performed to ensure the safe range of risk. Collected data from the FSCT indicate the capability of the car body to protect the vehicle occupants against injury during a collision. FSCT are expensive, time consuming and require sophisticated infrastructure. Therefore, numerical modelling and simulation are actively used to study car crashes. Simulation of vehicle crashworthiness has been evolving over the past 45 years. Prior to development of powerful computers, up until the early 1970s, crash studies relied almost exclusively on experimental full-scale testing. The earlier numerical methods used for vehicle crashworthiness were based on the use of the lumped masses and nonlinear springs. The models built with these

methods, known as lumped parameters models (LPM), used lumped masses to represent parts of the vehicle, such as engine block or the passenger compartment, considered rigid during the analysis, and the springs to represent the structural elements responsible for absorbing the deformation energy. Although outshined by the more sophisticated finite element modelling techniques discussed later in the text, the simple lumped parameters models are still used today, especially when it comes to reconstruction of the crash event. One of the earliest and successful examples of the use of LPM is the model developed by Kamal in 1970's for simulation of vehicle frontal crash at velocities between 0 and 30 mph (48 km/h) [1]. Various examples of use of LPM to vehicle crash reconstruction and evaluation of crashworthiness can be found in the literature.

When there is a progressive collapse of the vehicle structure during frontal crash, two basic requirements should be fulfilled for preventing death or serious injury to occupant. The first requirement ensures that occupants do not sustain injuries caused by too high inertia forces. It dictates that the parameters that characterize the inertia forces felt by the occupant are kept below the threshold values specified in the corresponding standards. The second requirement ensures that occupants are not getting clamped by the car structure during the crash event. To fulfill this requirement the car deformation need to be limited. The severity of cars deformation can be estimated by maximum dynamic crush, which is the maximum displacement of the car front with respect to its center of gravity [2]. Also according to the European Standard EN1317-1 [3], another indicator for potential injury during a crash event is the acceleration severity index(ASI), which is determined from the acceleration measurement closer to the center of gravity of the car. This indicator is described later in the text. In the past few decades, much research has been carried out in the field of vehicle crashworthiness using LPM which resulted in several novel computational models of vehicle collisions. In his book, Huang in [4], developed several mathematical models for vehicle crashworthiness using the LPM approach. Inspired by Huang 's work, Pawlus et al. [2,5] presented outstanding results for vehicle crashworthiness assessment using the LPM composed of springs, dampers and masses joined in various arrangements.

In [6], Marzbanrand expanded the Kalmal Model to a five-degrees of freedom (5-DOFs) lumped parameters model for the frontal crash and analyzed the response of occupant during the impact. In [7], the authors proposed an approach to control the seat belt restraint system force during a frontal crash to reduce thoracic injury. Klausen et al. [8,9] introduced a firefly optimization method to estimate parameters of vehicle crash test based on a single spring-mass-damper model. Ofochebe et al. in [10], studied the performance of vehicle front structure using a 5-DOFs lumped mass-spring model composed of body, engine, the cross-member, the suspension and the bumper masses. Munyazikwiye et al. in [11,12], introduced linear piecewise lumped parameters models and the genetic algorithm (GA) on the existing lumped parameters models to simulate a vehicle (accommodating an occupant) into barrier and a vehicle-to-vehicle frontal crashes, respectively. This GA has also been used in [13] for calculating the optimized parameters of a 12-DOFs model for two vehicle types in two different frontal crashes. Lim in [14,15], using SISAM software, presented various research results based on the extraction of lumped parameters model from the experimental data to reconstruct the vehicle crash kinematics. Recently, Mazurkiewicz et al. in [16] used the LPM to improve the safety of children transported in motor vehicles subjected to a side impact during a vehicle crash, while Vangi et al. [17] proposed a step-by-step procedure to collect data for a two vehicles accident reconstruction. In [18–20] the authors proposed an optimization procedure to assist multi-body vehicle model development for vehicle crashworthiness. Tso-Liang et al. in [19], examined the dynamic response of a human body in a crash event and assessed the injuries sustained to the occupant's head, chest and pelvic regions.

By the late 1980's explicit nonlinear finite element analysis (FEA), came into wide use following the development of powerful computers. While the first explicit finite element codes for research application appeared in the mid 1960s, the commercial explicit finite element codes came to use by the end of 1980s [21]. For example the company that distributes LS-DYNA [22] software used in this article was started by John Hallquist in 1989 [21]. Among the various vehicle crash simulation techniques,

explicit FEA is probably the most frequently used. In fact the first major area of application of explicit FEA was automotive crashworthiness.

Some examples of use of FEA for improvement of vehicle crashworthiness include the following: Cheng et al in [23], used LS-DYNA software to develop a single model that can be successfully used in computational simulations of full frontal, offset frontal, side, and oblique car-to-car impacts. In [24], an improvement of energy absorbing structure of a commercial vehicle for crashworthiness was achieved through FEA. Huiwen et al. [25,26], used an explicit code in LS-DYNA for the crash simulations of a full vehicle. In their model the vehicle body structure was first validated using experimental modal analysis in order to ensure that the distributed stiffness and mass of the model were equivalent to the actual body structure. Moradi et al. [27], proposed a FEM that can be utilized in the design process of a vehicle by reducing the aggressivity of the vehicle and increasing the on-road fleet compatibility in order to minimize the occupant injury. In [28], the authors developed a numerical model of a car crash by analysing the scenarios where a high-speed vehicle was crashing into a wall and a static vehicle. Their research objective was to identify the sources of harm to driver and passengers when car crashes occur. To assure a bumper design which meets the safety requirements, Kankariya and Sayyad in [29], used an explicit FEA to investigate stress and effective plastic strain of bumper at impact. Based on their simulation results, the modifications in bumper design to improve its impact performance were recommended. Recently, Hickey and his co-author in [30] conducted a quasi-static simulation of a 2002 Ford Explorer crash via FEA.

Finite element models are relatively complex and require large amount of computational time. The availability of simpler numerical tool for estimation of basic vehicle crashworthiness parameters can assist the designer and speed up the design process. Lumped parameters models might save as such tool. Primarily, LPMs have been used for vehicle crash reconstruction, but to the best of the authors' knowledge, their predictive capability has not yet been investigated elsewhere in literature. In this paper, the authors investigated whether it is possible to accurately estimate basic crashworthiness parameters such as maximum dynamic crush and ASI, using the earlier proposed LPM [11,12] instead of the commonly used explicit FE model. To this end, the proposed piecewise LPM was calibrated, using the crash data and the Genetic algorithm and validated by comparing its predictions with the FEA simulation results for different crash velocities.

2. Materials and Methods

A full-scale crash test of a Ford Taurus (2004 model) in Figure 1 is chosen as a base line for the LPM and FEA used in this paper. The test weight and impact speed of the vehicle were 1739 kg and 55.9 km/h, respectively. The experimental data and finite element analysis model input were obtained from NHTSA open database [31].

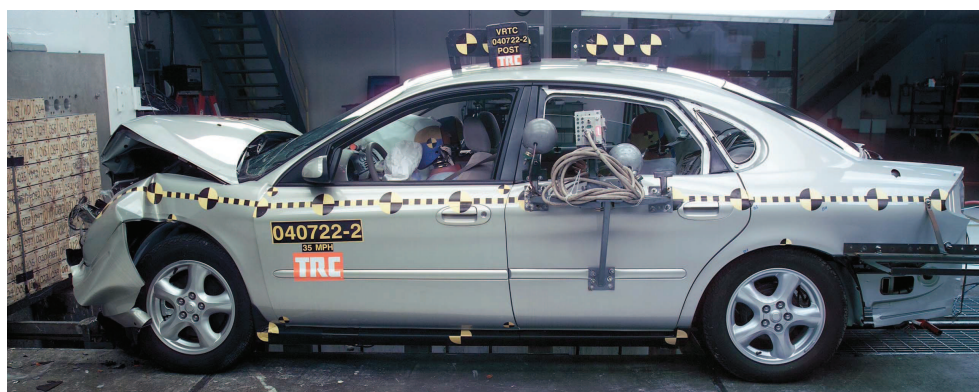


Figure 1. Full-scale crash test of a Ford Taurus (2004 model) at 56 km/h [31].

2.1. Experimental data and signal filtering

Fourier transform and filters are useful tools for processing and analyzing discrete data. The filtering starts with the identification of frequency components in a signal. A low pass filter allows low frequency components to pass but high components are truncated. To identify frequency components, the Fourier transformation is performed on a time domain signal in order to estimate the cut-off frequency used for the low pass filter. The Fourier transform (FT) of a function $x(t)$ also called the spectrum of $x(t)$, denoted $X(\omega)$ and the inverse Fourier transform exist if the Fourier transform pair, as referred to [32] in equation (1), holds. That is:

$$X(\omega) = \int_{-\infty}^{\infty} x(t)e^{-j\omega t} dt \xleftrightarrow{FT} x(t) = \frac{1}{2\pi} \int_{-\infty}^{\infty} X(\omega)e^{j\omega t} d\omega \quad t, \omega \in \mathbb{R}. \quad (1)$$

The transformation pair in (1) holds if $x(t)$ and $X(\omega)$ are defined and finite for all $\omega \in \mathbb{R}$ and $t \in \mathbb{R}$. The time and frequency domain pair transformation is computed using the fast Fourier transform and the inverse fast Fourier transform, respectively. If a continuous-time system is linear and time-invariant, the output $y(t)$ is related to the input $x(t)$ by a convolution integral [32] between the two functions $x(t)$ and $h(t)$ and is define as

$$y(t) = (Hx)(t) = (h \otimes x)(t) = \int_{-\infty}^{\infty} x(\tau)h(t - \tau)d\tau = h(t) \otimes x(t) \quad (2)$$

or equivalently in the discrete-time case, by the convolution sum, if $x(n)$ is an N point signal running from 0 to N and $h[n]$ is an M point signal running from 0 to M , the convolution of the two signals is a difference equation of the form,

$$y[n] = h[n] \otimes x[n] = \sum_{k=0}^M h[k]x[n - k] \quad (3)$$

where $h(t)$ or $h[n]$ is the impulse response of the system [33]. The symbol \otimes is a circular convolution operator.

In this paper, the acceleration signal (experimental data) is filtered using a Finite Impulse Response (FIR) filter before performing numerical integration to obtain the velocity and displacement responses, respectively.. Figure 2 shows the noisy and filtered acceleration signals for a vehicle crashing into a barrier. A cut-off frequency of 0.5 kHz with a sampling rate of 10 KHz are chosen while designing a suitable low pass filter. A filter order of 30 and a Kaiser window type are used for the filtering process.

2.2. Linear piecewise lumped parameters model

The model consists of a Kelvin model shown in Figure 3. In line of the model development, the dynamical model proposed in [4] for the free vibration analysis is adopted for solving the impact responses. Then, the genetic algorithm is used to estimate and optimize the model parameters. At time of crush, the built up spring and damping forces are defined as

$$F_k = k(x) \cdot x, \quad (4a)$$

$$F_c = c(\dot{x}) \cdot \dot{x}, \quad (4b)$$

and the dynamic equation of the model in Figure 3 as

$$\ddot{x} = (-F_k - F_c)/m \quad (5)$$

where \dot{x} and x are the velocity and displacement of the center of gravity of mass m (the mass of the vehicle).

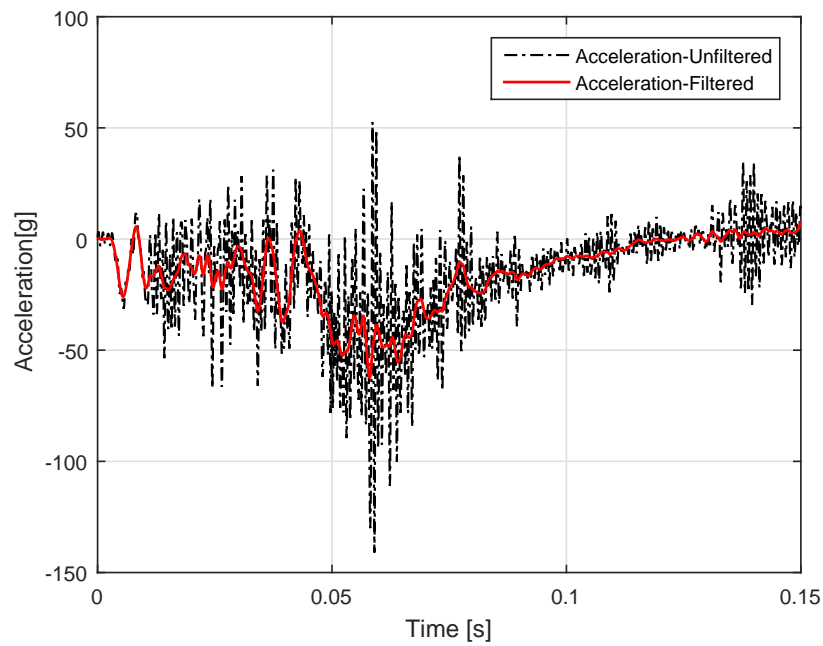


Figure 2. Noisy and Filtered acceleration signals for full-scale frontal crash

146 2.3. Piecewise linear approximations for springs and dampers

147 The spring stiffness and damping coefficients in the model, described in the previous section, are
 148 defined by the linear piecewise functions in equations (6a) - (6b).

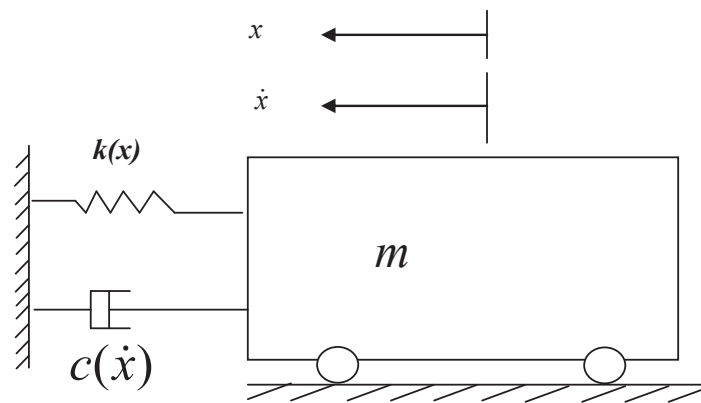


Figure 3. Lumped parameter model

$$k(x) = \begin{cases} k_1 + \frac{k_2 - k_1}{x_1} x & x \leq x_1 \\ k_2 + \frac{k_3 - k_2}{x_2 - x_1} (x - x_1) & x_1 \leq x \leq x_2 \\ k_3 + \frac{k_4 - k_3}{1m - x_2} (x - x_2) & x_2 \leq x \leq 1m \end{cases} , \quad (6a)$$

$$c(\dot{x}) = \begin{cases} c_1 - \frac{c_1 - c_2}{\dot{x}_1} \dot{x} & \dot{x} \leq \dot{x}_1 \\ c_2 - \frac{c_2 - c_3}{\dot{x}_2 - \dot{x}_1} (\dot{x} - \dot{x}_1) & \dot{x}_1 \leq \dot{x} \leq \dot{x}_2 \\ c_3 - \frac{c_3 - c_4}{v_0 - \dot{x}_2} (\dot{x} - \dot{x}_2) & \dot{x}_2 \leq \dot{x} \leq 25m/s \end{cases}, \quad (6b)$$

where C_m is the value of the maximum dynamic crush or the maximum deformation of the vehicle's front structure.

The upper limits of $1m$ and $25m/s$ in equations (6a) and (6b), are the guess values based on the expected range of deformations and velocities, respectively.

2.4. Calibration scheme using the genetic algorithm

A genetic algorithm (GA), is a method used for solving problems based on natural selection. The GA is applied to solve a variety of optimization problems that are not well suited for standard optimization algorithms, including problems in which the objective function is discontinuous, nondifferentiable, stochastic, or highly nonlinear [34]. This algorithm repeatedly modifies a population of individual solutions. At each step, the genetic algorithm selects individuals at random from the current population to be parents and uses them to produce the children for the next generation. Over successive generations, the population evolves toward an optimal solution. This evolutionary algorithm holds a population of individuals (chromosomes), which evolve by means of selection and other operators like crossover and mutation. Every individual in the population gets an evaluation of its adaptation (fitness) to the environment. The selection chooses the best gene combinations, which through crossover and mutation, should drive to better solutions in the next population [35]. The algorithm for solving the problem defined by equation (5) is shown in Figure 4. The GA-type of search schemes is function-value comparison-based, with no derivative computation. It attempts to move points through a series of generations, each being composed of a population which has a set number (population size, 200 in this work) and 12 individuals or parameters (four stiffness values, four damping coefficient values, two position values, x_1 and x_2 , two intermediate velocities \dot{x}_1 and \dot{x}_2). The proposed algorithm seeks to find the minimum function between several variables as can be stated in a general form $\min f(p)$, where p denotes the unknown variables in the model. In this paper, the cost function to be minimized is the norm of the absolute error between the displacement, velocity and acceleration of the simulated cash and the FEA or full-scale crash test data and is defined as:

$$\begin{aligned} |Error_1| &= \text{sum}(|E_{Est} - E_{Exp}|^T \times |E_{Est} - E_{Exp}|) \\ |Error_2| &= \text{sum}(|E_{Est} - E_{FEA}|^T \times |E_{Est} - E_{FEA}|) \end{aligned} \quad (7)$$

where E_{Est} , E_{Exp} and E_{FEA} are the model, experimental and FEA variables (displacement, velocity and acceleration) respectively and "T" stands for transpose.

An initial guess of parameters is chosen and substituted in the piecewise linear functions defined equations (6a) and (6b). Then, the obtained spring stiffness and damping coefficients are substituted into equations (4a) and (4b), which are respectively substituted in the dynamic equation (5). Finally, equation (5) is numerically solved to get the simulated kinematic results. These kinematic results are compared with the time-history from the full-scale crash test and FEA, respectively. The cost function in Equation (7) is evaluated, and when the cost function is minimum the solver terminates, otherwise the GA keeps on tuning the model parameters to match the experimental results or FEA results.

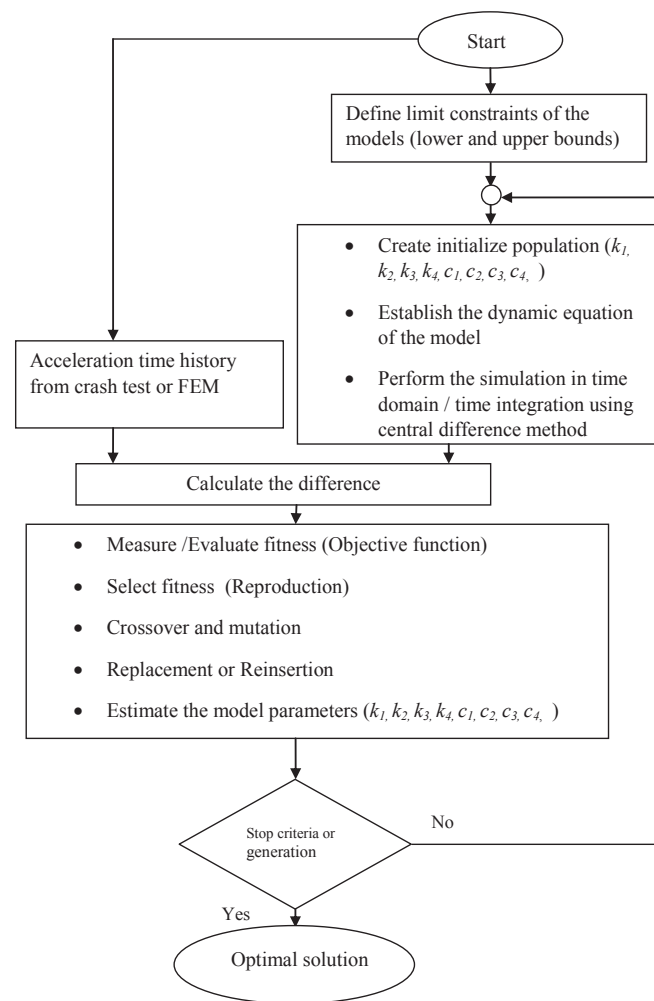


Figure 4. Calibration procedure using genetic algorithm

2.5. Finite element analysis

As mentioned earlier, the input to finite element analysis was obtained from the National Highway Traffic Safety and Administration (NHTSA) open Database [31]. The following is a summary describing the studied FEM:

- Number of parts : 804
- Number of nodes : 922007
- Number of beam elements : 10
- Number of shell elements : 838926
- Number of solid elements : 134468

The simulations were performed using the LS-DYNA software Version R8.10 (Revision R8.105896). The impact velocities of 40, 48, 56, 64 and 72 km/h were simulated and the average computational time per each simulation was about 14 hours. Acceleration data were recorded at the center of gravity (CG) of the finite element model.

In case when the finite element analysis uses under-integrated shell and solid elements, non-physical, zero-energy deformations modes such as hourglass modes might occur. Some small amount of hourglass energy can be tolerated, but this non-physical deformation mode need to be kept under control. The ratio of the hourglass energy to the internal energy should not exceed the

recommended value. In the presented analysis, this ratio was carefully controlled and kept below 0.01, which is the recommended value according to [22,36].

2.6. Acceleration Severity Index (ASI)

The ASI is intended to give a measure of the severity of inertia force experienced by a person seated in the proximity of the CG of the vehicle during impact with flexible barriers. The ASI is derived from the acceleration time-histories measured at the CG of the impacting vehicle and is computed as follows [37]:

$$ASI(t_i) = \sqrt{\left(\frac{\bar{a}_x}{\hat{a}_x}\right)^2 + \left(\frac{\bar{a}_y}{\hat{a}_y}\right)^2 + \left(\frac{\bar{a}_z}{\hat{a}_z}\right)^2} \quad (8)$$

where $\hat{a}_x = 12g$, $\hat{a}_y = 9g$, $\hat{a}_z = 10g$ are limit values for the components of the acceleration along the body axes x (longitudinal direction), y (lateral direction) and z (vertical direction), respectively. These values are obtained from the human body tolerances limits, interpreted as the values below which passenger risk is very small (light injury if any) and $g = 9.81m/s^2$ is the acceleration due to gravity, while $\bar{a}_x, \bar{a}_y, \bar{a}_z$ are the components of acceleration of a selected point close to CG of the vehicle, averaged over a moving time interval $\delta = 0.050$ seconds and the ASI is the maximum value of ASI(t). The average acceleration components are defined in equation (9).

$$\begin{aligned} \bar{a}_x &= \frac{1}{\delta} \int_t^{t+\delta} a_x dt \\ \bar{a}_y &= \frac{1}{\delta} \int_t^{t+\delta} a_y dt \\ \bar{a}_z &= \frac{1}{\delta} \int_t^{t+\delta} a_z dt \end{aligned} \quad (9)$$

According to the European standard EN 1317-2:2010 [38], three impact severity levels are classified as A, B and C classes for flexible road safety barriers, and the respective recommended values of ASI for each class are:

- Class A: $ASI \leq 1$
- Class B: $1.0 \leq ASI \leq 1.4$
- Class C: $1.4 \leq ASI \leq 1.9$

The impact Severity Class A affords a greater level of comfort for vehicle occupants than Class B and C. The more the ASI exceeds unity, the more the impact consequences for the passengers are dangerous [39].

In case of a full frontal crash, the acceleration components in the lateral and vertical directions are less significant as compared to the longitudinal acceleration. Hence, in this work, the computation of ASI involves only the longitudinal component and its associated 12g threshold acceleration. That is:

$$ASI = \frac{|\bar{a}_x|}{12} \quad (10)$$

The calculation of ASI is based on the velocity curves obtained from the vehicle's center of gravity. The procedure to compute the longitudinal ASI is adapted from [40]:

1. Using the measured vehicle crash velocity data, calculate the 0.050 s average acceleration values by computing the difference in velocity at points 0.050 s apart and dividing by 0.050 s. The 0.050 s moving average longitudinal acceleration, $\bar{a}_x(t_i)$, can also be computed as follows:

$$\bar{a}_x(t_i) = \frac{\sum_{t=i-0.05}^i a_{t_i}}{\delta} = \frac{\sum_0^i a_{t_i} - \sum_0^{i-0.05} a_{t_i}}{\delta} = \frac{v_{t=i} - v_{t=i-0.05}}{0.05} \quad (11)$$

- 231
- 232
- 233
- 234
- 235
- 236
- 237
- 238
- 239
- 240
- 241
- 242
- 243
- 244
- 245
- 246
- 247
- 248
- 249
- 250
- 251
- 252
- 253
- 254
- 255
- 256
- 257
- 258
- 259
- 260
- 261
- 262
- 263
- 264
- 265
- 266
- 267
- 268
- 269
- 270
- 271
- 272
- 273
- 274
- 275
- 276
- 277
- 278
- 279
- 280
- 281
- 282
- 283
- 284
- 285
- 286
- 287
- 288
- 289
- 290
- 291
- 292
- 293
- 294
- 295
- 296
- 297
- 298
- 299
- 300
- 301
- 302
- 303
- 304
- 305
- 306
- 307
- 308
- 309
- 310
- 311
- 312
- 313
- 314
- 315
- 316
- 317
- 318
- 319
- 320
- 321
- 322
- 323
- 324
- 325
- 326
- 327
- 328
- 329
- 330
- 331
- 332
- 333
- 334
- 335
- 336
- 337
- 338
- 339
- 340
- 341
- 342
- 343
- 344
- 345
- 346
- 347
- 348
- 349
- 350
- 351
- 352
- 353
- 354
- 355
- 356
- 357
- 358
- 359
- 360
- 361
- 362
- 363
- 364
- 365
- 366
- 367
- 368
- 369
- 370
- 371
- 372
- 373
- 374
- 375
- 376
- 377
- 378
- 379
- 380
- 381
- 382
- 383
- 384
- 385
- 386
- 387
- 388
- 389
- 390
- 391
- 392
- 393
- 394
- 395
- 396
- 397
- 398
- 399
- 400
- 401
- 402
- 403
- 404
- 405
- 406
- 407
- 408
- 409
- 410
- 411
- 412
- 413
- 414
- 415
- 416
- 417
- 418
- 419
- 420
- 421
- 422
- 423
- 424
- 425
- 426
- 427
- 428
- 429
- 430
- 431
- 432
- 433
- 434
- 435
- 436
- 437
- 438
- 439
- 440
- 441
- 442
- 443
- 444
- 445
- 446
- 447
- 448
- 449
- 450
- 451
- 452
- 453
- 454
- 455
- 456
- 457
- 458
- 459
- 460
- 461
- 462
- 463
- 464
- 465
- 466
- 467
- 468
- 469
- 470
- 471
- 472
- 473
- 474
- 475
- 476
- 477
- 478
- 479
- 480
- 481
- 482
- 483
- 484
- 485
- 486
- 487
- 488
- 489
- 490
- 491
- 492
- 493
- 494
- 495
- 496
- 497
- 498
- 499
- 500
- 501
- 502
- 503
- 504
- 505
- 506
- 507
- 508
- 509
- 510
- 511
- 512
- 513
- 514
- 515
- 516
- 517
- 518
- 519
- 520
- 521
- 522
- 523
- 524
- 525
- 526
- 527
- 528
- 529
- 530
- 531
- 532
- 533
- 534
- 535
- 536
- 537
- 538
- 539
- 540
- 541
- 542
- 543
- 544
- 545
- 546
- 547
- 548
- 549
- 550
- 551
- 552
- 553
- 554
- 555
- 556
- 557
- 558
- 559
- 560
- 561
- 562
- 563
- 564
- 565
- 566
- 567
- 568
- 569
- 570
- 571
- 572
- 573
- 574
- 575
- 576
- 577
- 578
- 579
- 580
- 581
- 582
- 583
- 584
- 585
- 586
- 587
- 588
- 589
- 590
- 591
- 592
- 593
- 594
- 595
- 596
- 597
- 598
- 599
- 600
- 601
- 602
- 603
- 604
- 605
- 606
- 607
- 608
- 609
- 610
- 611
- 612
- 613
- 614
- 615
- 616
- 617
- 618
- 619
- 620
- 621
- 622
- 623
- 624
- 625
- 626
- 627
- 628
- 629
- 630
- 631
- 632
- 633
- 634
- 635
- 636
- 637
- 638
- 639
- 640
- 641
- 642
- 643
- 644
- 645
- 646
- 647
- 648
- 649
- 650
- 651
- 652
- 653
- 654
- 655
- 656
- 657
- 658
- 659
- 660
- 661
- 662
- 663
- 664
- 665
- 666
- 667
- 668
- 669
- 670
- 671
- 672
- 673
- 674
- 675
- 676
- 677
- 678
- 679
- 680
- 681
- 682
- 683
- 684
- 685
- 686
- 687
- 688
- 689
- 690
- 691
- 692
- 693
- 694
- 695
- 696
- 697
- 698
- 699
- 700
- 701
- 702
- 703
- 704
- 705
- 706
- 707
- 708
- 709
- 710
- 711
- 712
- 713
- 714
- 715
- 716
- 717
- 718
- 719
- 720
- 721
- 722
- 723
- 724
- 725
- 726
- 727
- 728
- 729
- 730
- 731
- 732
- 733
- 734
- 735
- 736
- 737
- 738
- 739
- 740
- 741
- 742
- 743
- 744
- 745
- 746
- 747
- 748
- 749
- 750
- 751
- 752
- 753
- 754
- 755
- 756
- 757
- 758
- 759
- 760
- 761
- 762
- 763
- 764
- 765
- 766
- 767
- 768
- 769
- 770
- 771
- 772
- 773
- 774
- 775
- 776
- 777
- 778
- 779
- 780
- 781
- 782
- 783
- 784
- 785
- 786
- 787
- 788
- 789
- 790
- 791
- 792
- 793
- 794
- 795
- 796
- 797
- 798
- 799
- 800
- 801
- 802
- 803
- 804
- 805
- 806
- 807
- 808
- 809
- 810
- 811
- 812
- 813
- 814
- 815
- 816
- 817
- 818
- 819
- 820
- 821
- 822
- 823
- 824
- 825
- 826
- 827
- 828
- 829
- 830
- 831
- 832
- 833
- 834
- 835
- 836
- 837
- 838
- 839
- 840
- 841
- 842
- 843
- 844
- 845
- 846
- 847
- 848
- 849
- 850
- 851
- 852
- 853
- 854
- 855
- 856
- 857
- 858
- 859
- 860
- 861
- 862
- 863
- 864
- 865
- 866
- 867
- 868
- 869
- 870
- 871
- 872
- 873
- 874
- 875
- 876
- 877
- 878
- 879
- 880
- 881
- 882
- 883
- 884
- 885
- 886
- 887
- 888
- 889
- 890
- 891
- 892
- 893
- 894
- 895
- 896
- 897
- 898
- 899
- 900
- 901
- 902
- 903
- 904
- 905
- 906
- 907
- 908
- 909
- 910
- 911
- 912
- 913
- 914
- 915
- 916
- 917
- 918
- 919
- 920
- 921
- 922
- 923
- 924
- 925
- 926
- 927
- 928
- 929
- 930
- 931
- 932
- 933
- 934
- 935
- 936
- 937
- 938
- 939
- 940
- 941
- 942
- 943
- 944
- 945
- 946
- 947
- 948
- 949
- 950
- 951
- 952
- 953
- 954
- 955
- 956
- 957
- 958
- 959
- 960
- 961
- 962
- 963
- 964
- 965
- 966
- 967
- 968
- 969
- 970
- 971
- 972
- 973
- 974
- 975
- 976
- 977
- 978
- 979
- 980
- 981
- 982
- 983
- 984
- 985
- 986
- 987
- 988
- 989
- 990

3. Results

The spring stiffness and damping coefficient characteristics of the vehicle’s front structure, optimized through the GA, are shown in Table 1.

Table 1. Estimated structural parameters of the vehicle frontal crash model calibrated at 56 km/h

Parameters	LPM calibrated to FSCT	LPM calibrated to FEM
Stiffness [N/m]		
k_1	7195 N/m	25718 N/m
k_2	7210 N/m	31444 N/m
k_3	25386 N/m	45476 N/m
k_4	711060 N/m	467830 N/m
Damping [Ns/m]		
c_1	59444 Ns/m	80827 Ns/m
c_2	51590 Ns/m	7775 Ns/m
c_3	4997 Ns/m	38812 Ns/m
c_4	1382 Ns/m	5703 Ns/m

Figure 5 illustrates three out of five FEA simulations of a Ford-Taurus (2004 model) crashing into a fixed rigid wall at initial velocities of 40, 56 and 72 km/h, respectively. The kinematic time-history (displacements, velocities and accelerations) are compared as shown in Figures 6 to 8. These Figures show the predictions of the LPM for a range of speeds (40, 48, 56, 64 and 72 km/h, respectively). Figures 8a and 8b, present a summary of kinematics results of the LPM calibrated at 56 km/h against the full-scale crash test and FEA, respectively. The crashworthiness parameters in terms of maximum dynamic crush (C_m), time of crush (t_m) and ASI for the range of velocities are summarized in Table 2.

4. Discussion

LPM tries to reconstruct the crash event using the damping and stiffness. The stiffness is initially low at time of contact with the barrier and increases piece-wisely until the car frontal structure plastically deforms at the dynamic crush. This apparent increase of stiffness is due to compaction of many elements that buckle together when the front structure of the car is completely compressed at the maximum dynamic crush. The vehicle’s frontal structure absorbs the energy and deforms sufficiently. From Figure 5, hood and the fender are completely bent, the bumper is plastically deformed at high impact velocity (72 km/h). It is noted that the maximum deviation from the FEA dynamic crush, C_m , is less than 3 cm. There is a reasonable agreement between the values of injury indicators from the LPM and FEA. The LPM fits very well up to the maximum dynamic crush, but during the rebound phase the displacement of the LPM starts deviating from what is observed in the full-scale crash test as shown in Figure 6. At velocities below the calibration point, a deviation is observed just after the time of crush, during the rebound phase, when the LPM is calibrated to FEA as shown in Figure 8b. These Figures show the results of deformation modes going from buckling and bending to compression of the crushed structure.

For different impact velocities, small deviations between the results from LPM calibrated to FEM and FSCT are observed. This is evidenced by the dynamic crushes with their respective time of occurrence and the rebound velocities. The main influencing parameter characterizing the crash severity is the maximum dynamic crush (C_m), which describes the highest car’s deformation. It is noted from Table 2 that the ASI for LPM and FEM are almost similar at a specific impact velocity. The estimated parameters show that the level of accident severity is high when the impacting velocity of the vehicle is greater than 48 km/h. The high values of ASI reported in this work could be due to the rigidity of the barrier, since the range of ASI mentioned earlier has been defined for flexible barriers.

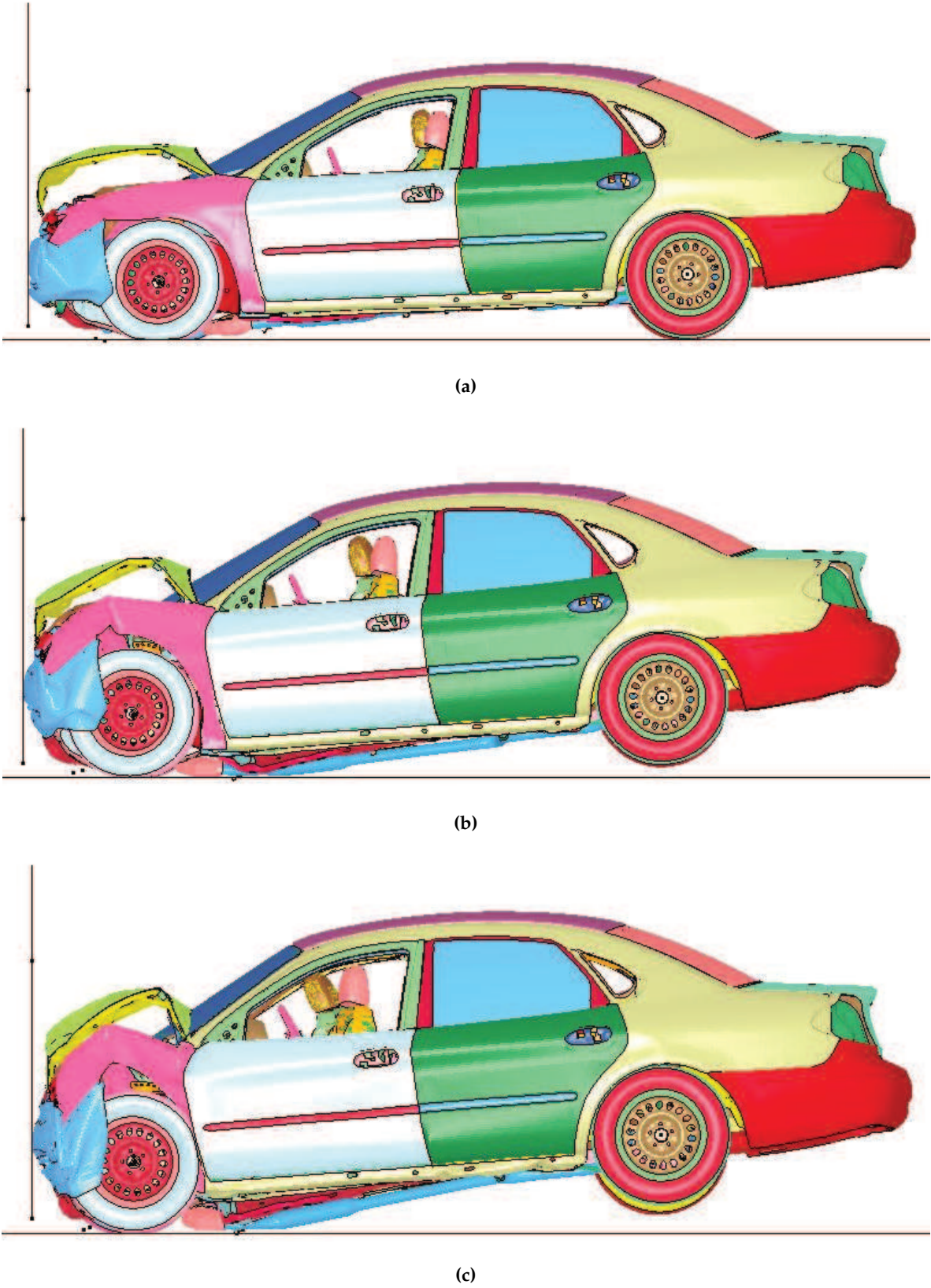


Figure 5. Deformed vehicle frontal structure through FEA at impact velocities of (a) 40 km/h, (b) 56 km/h and (c) 72 km/h

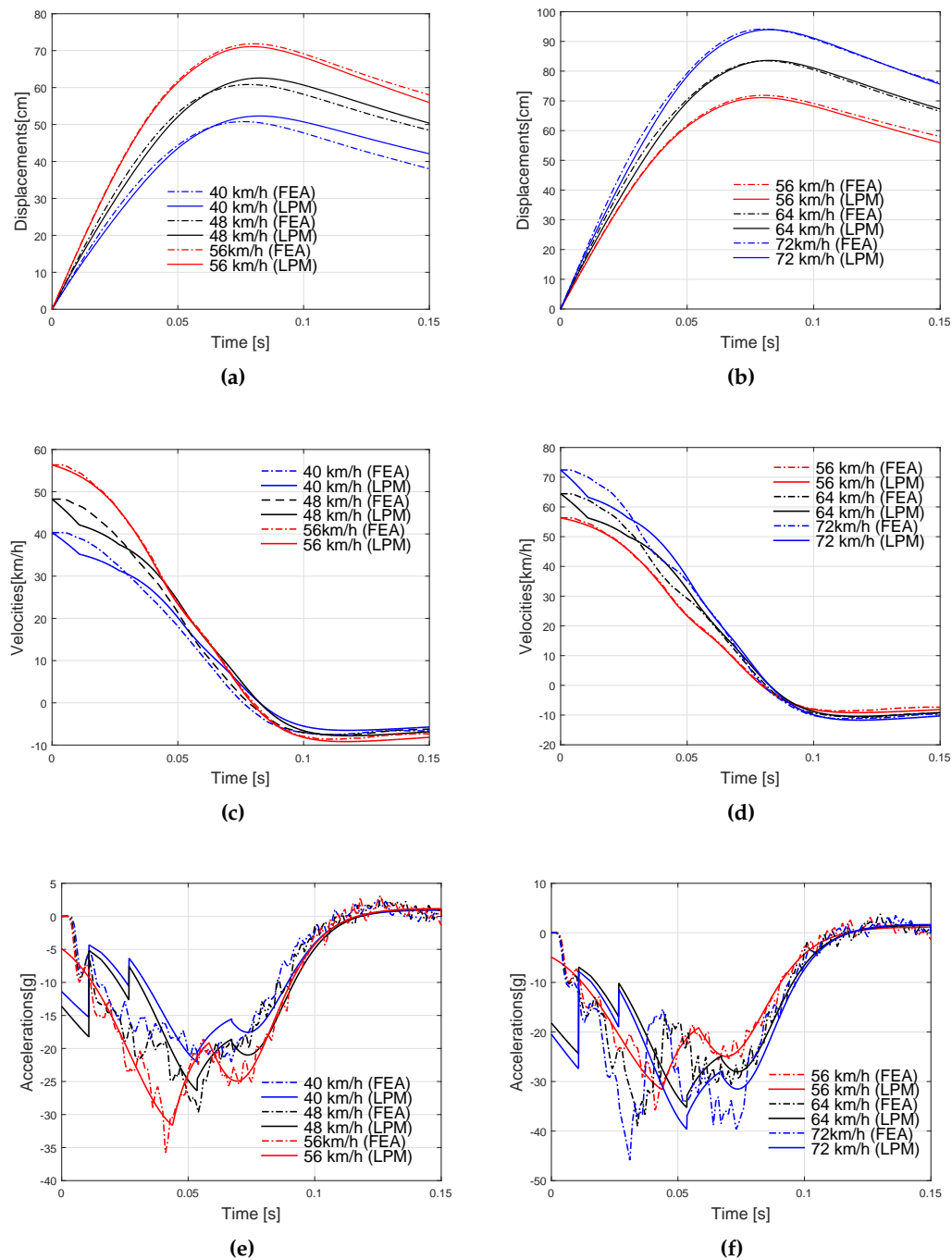


Figure 6. Displacement, velocity and acceleration plots comparison in case of LPM calibrated to FEA, (a), (c) and (e) impact velocities lower than the calibration point (56 km/h); (b), (d) and (f) impact velocities higher than the calibration point.

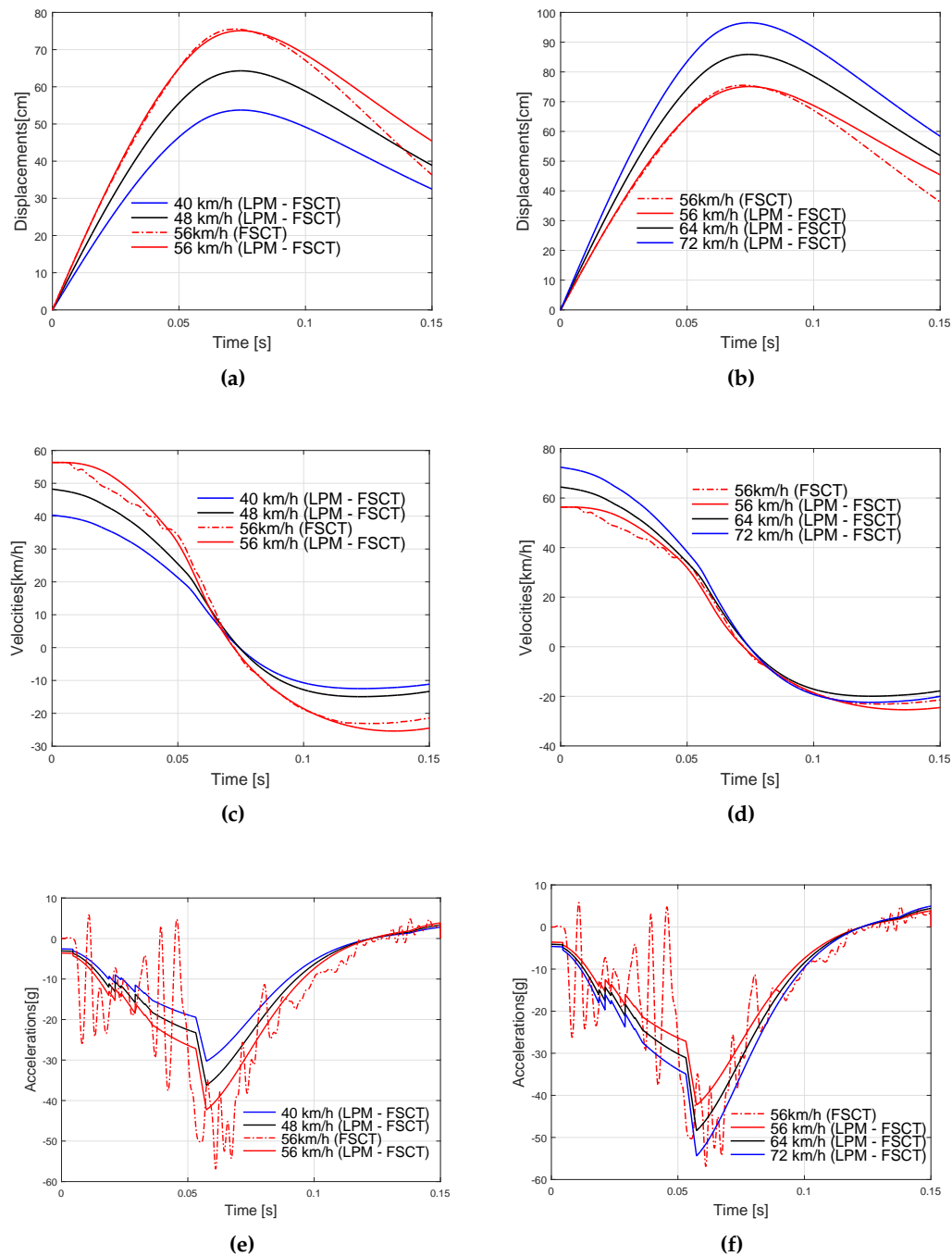
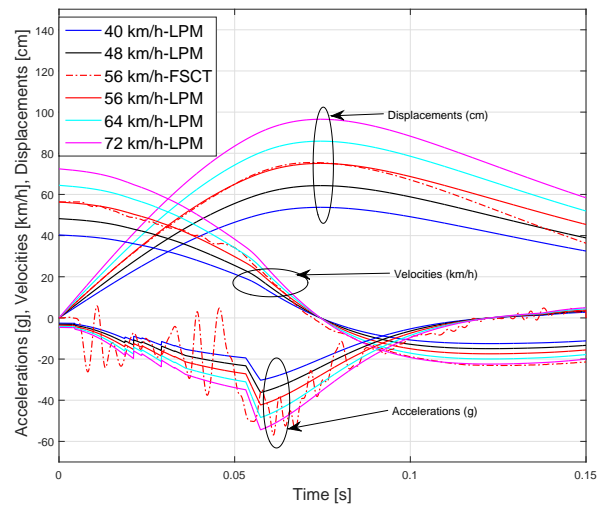
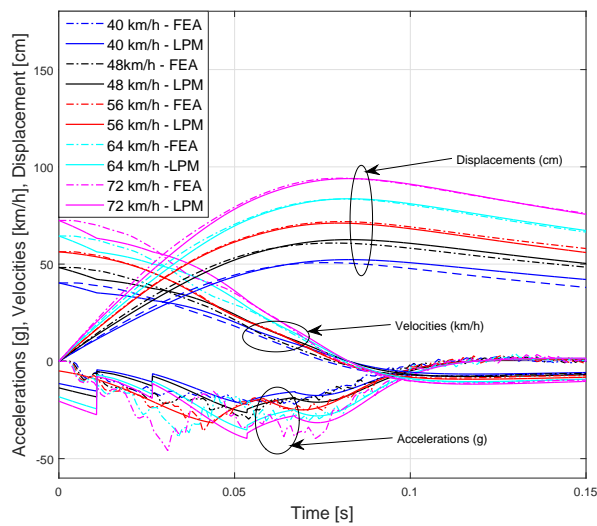


Figure 7. Displacement, velocity and acceleration plot comparison in case of LPM calibrated to FSCT, (a), (c) and (e) impact velocities lower than the calibration point (56 km/h); (b), (d) and (f) impact velocities higher than the calibration point.



(a)



(b)

Figure 8. A summary of kinematic time histories for (a) LPM calibrated to FSCT and (b) LPM calibrated to FEA.

Table 2. Estimated crashworthiness parameters for FSCT, FEA and LPM.

Approaches	Parameters	Impact velocities				
		40 km/h	48 km/h	56 km/h ^c	64 km/h	72 km/h
FSCT	t_m [s]	-	-	0.0723	-	-
	C_m [m]	-	-	0.7551	-	-
	ASI [-]	-	-	2.5	-	-
LPM calibrated to FSCT	t_m [s]	0.0736	0.0740	0.0738	0.0741	0.0741
	C_m [m]	0.5373	0.6429	0.7508	0.8588	0.9653
	ASI [-]	1.7	2.1	2.6	2.7	3.1
FEA	t_m [s]	0.0755	0.0781	0.0801	0.0804	0.0800
	C_m [m]	0.5077	0.6077	0.7180	0.8331	0.9408
	ASI [-]	1.5	1.8	2.0	2.3	2.5
LPM calibrated to FEA	t_m [s]	0.0824	0.0825	0.0793	0.0822	0.0805
	C_m [m]	0.5231	0.6258	0.7108	0.8360	0.9396
	ASI [-]	1.4	1.6	2.0	2.3	2.5

^cCalibration point, t_m is the time at maximum dynamic crush, C_m is the maximum dynamic crush and ASI is the acceleration severity index.

The results show that, the LPM agrees with the experimental data and the conventional FEA, and the computational time for the LPM is between 15 and 30 minutes while the average computational time for the FEA is 14 hours excluding the undefined time spent in developing the complex FEM of a complete vehicle.

5. Conclusions

It is obvious that simple LPM cannot replace complex FE model with regard to crash simulations, but it can greatly assist to speed up the analysis. Due to complexity of the FEM, the analyst typically needs several iterations with adjustment of simulation parameters before a successful simulation is produced. Typically three to five iterations are necessary, each taking about half of the full simulation time before the analysis termination. Hence to produce a single successful FE-analysis of the crash event requires about a week of working time. To produce a N number of successful FE-simulations for a range of velocities would typically take less time than N-weeks since once a successful combination of parameters is found, it can be used for most of simulations and only minor adjustments are needed for different velocities. In the current study, the FE analysis for the five different velocities was produced within a month. Using a LPM allows to perform one FEA instead of five, calibrate the LPM to FEM and obtain the estimate of the crash parameters for a range of velocities. Hence LPM approach extracts a month work within a week. Thus the piecewise LPM seems to be a promising tool in design process as evidenced by its predictive capability with less computation time.

The extension of this work could be the consideration of the predictive capabilities of the LPM for other crash scenarios such as oblique crash, side impact and vehicle-to-vehicle crash respectively.

Author Contributions: Bernard B. Munyazikwiye, the main author, proposed the approach, processed the data, analysed the results and wrote the article; Dmitry Vysochinskiy and Kjell G. Robbersmyr, scientific advisers, supervised the work and revised the article; Mikhail Khadyko, performed the FEA and the final revision of the article.

Conflicts of Interest: The authors declare no conflict of interest. The research is part of the main author's PhD-project and is funded by the University of Agder.

References

1. M.Kamal, M. Analysis and Simulation of Vehicle to Barrier Impact. *SAE International*, Technical Paper 1970, pp. 1 – 6.

2. Pawlus, W.; Karimi, H.R.; Robbersmyr, K.G. Development of lumped-parameter mathematical models for a vehicle localized impact. *Journal of Mechanical Science and Technology* **2011**, *25*, 1737–1747.
3. European Standard EN 1317. Road restraint systems, Terminology and general criteria for test methods. Technical report, European Committee of Standardization, 2010.
4. Huang, M. *Vehicle Crash Mechanics*, 1st ed.; CRC PRESS: Boca Raton, FL, USA, 2002.
5. Pawlus, W.; Nielsen, J.E.; Karimi, H.R.; Robbersmyr, K.G. Application of viscoelastic hybrid models to vehicle crash simulation. *International Journal of Crashworthiness* **2011**, *55*, 369 – 378.
6. Marzbanrad, J.; Pahlavani, M. Calculation of vehicle-lumped model parameters considering occupant deceleration in frontal crash. *International Journal of Crashworthiness* **2011**, *16*, 439 – 455.
7. Alnaqi, A.; Yigit, A. Dynamic Analysis and Control of Automotive Occupant Restraint Systems. *Jordan Journal of Mechanical and Industrial Engineering* **2011**, *5*, 39 – 46.
8. Klausen, A.; Tørdal, S.S.; Karimi, H.R.; Robbersmyr, K.G.; Jecmenica, M.; Melteig, O. Firefly Optimization and Mathematical Modeling of a Vehicle Crash Test Based on Single-Mass. *Journal of Applied Mathematics* **2014**, pp. 1 – 10. Article ID 150319.
9. Klausen, A.; Tørdal, S.S.; Karimi, H.R.; Robbersmyr, K.G. Mathematical Modeling and Numerical Optimization of Three Vehicle Crashes using a Single-Mass- Lumped Parameter Model. 24th International Technical Conference on the Enhanced Safety of Vehicles (ESV), Gothenburg , Sweden 8-11 June, 2015.
10. Ofochebe, S.M.; Ozoegwu, C.G.; Enibe, S.O. Performance evaluation of vehicle front structure in crash energy management using lumped mass spring system. *Advanced Modeling and Simulation in Engineering* **2015**, *2*, 1–18.
11. Munyazikwiye, B.B.; Karimi, H.R.; Robbersmyr, K.G. A Mathematical Model for Vehicle-Occupant Frontal Crash using Genetic Algorithm. 2016 UKSim-AMSS 18th International Conference on Computer Modelling and Simulation, Cambridge, United Kingdom, 6-8 April, 2016.
12. Munyazikwiye, B.B.; Karimi, H.R.; Robbersmyr, K.G. Optimization of Vehicle-to-Vehicle Frontal Crash Model Based on Measured Data Using Genetic Algorithm. *IEEE Access, Special Section on Recent Advances on Modelling, Optimization, and Signal Processing Methods in Vehicle Dynamics and Crash-worthiness* **2017**, *5*, 3131–3138.
13. Pahlavani, M.; Marzbanrad, J. Crashworthiness study of a full vehicle-lumped model using parameters optimization. *International Journal of Crashworthiness* **2015**, *20*, 573 – 591.
14. Lim, J.M. A Consideration on the Offset Frontal Impact Modeling Using Spring-Mass Model. *International Journal of Mechanical, Aerospace, Industrial, Mechatronic and Manufacturing Engineering* **2015**, *9*, 1453 – 1458.
15. Lim, J.M. Lumped Mass-Spring Model Construction for Crash Analysis using Full Frontal Impact Test Data. *International Journal of Automotive Technology* **2017**, *18*, 463 – 472.
16. Mazurkiewicz, L.; Baranowski, P.; Karimi, H.R.; Damaziak, K.; Malachowski, J.; Muszynski, A.; Muszynski, A.; Robbersmyr, K.G.; Vangi, D. Improved child-resistant system for better side impact protection. *Int J Adv Manuf Technol* **2018**, pp. 1–11.
17. Vangi, D.; Cialdai, C.; Gulino, M.S.; Robbersmyr, K.G. Vehicle Accident Databases: Correctness Checks for Accident Kinematic Data. *Designs* **2018**, *2*, 1–11.
18. Sousa, L.; P.Verssimo.; Ambrsio, J. Development of generic multibody road vehicle models for crashworthiness. *Multibody Syst Dyn* **2008**, *19*, 133 – 158.
19. Teng, T.; Chang, F.; Liu, Y.; Peng, C. Analysis of dynamic response of vehicle occupant in frontal crash using multibody dynamics method. *Mathematical and Computer Modelling* **2008**, *48*, 1724 – 1736.
20. Carvalho, M.; Ambrsio, J.; Eberhard, P. Identification of validated multibody vehicle models for crash analysis using a hybrid optimization procedure. *Struct Multidisc Optim* **2011**, *44*, 85 – 97.
21. Belytschko, T.; Liu, W.K.; Moran, B.; Elkhodary, K.I. *Nonlinear Finite Elements for Continua and Structures*; John Wiley and Sons, 2014.
22. Livermore Software Technology Corporation, Livermore, California 94551-0712. *LS-DYNA Keyword User's Manual, VOLUME II*, ls-dyna r9.0 ed., 2016.
23. Cheng, Z.; Thacker, J.; Pilkey, W.; Hollowell, W.; Reagan, S.; Sieveka, E. Experiences in reverse-engineering of a finite element automobile crash model. *Finite Elements in Analysis and Design* **2001**, *37*, 843 – 860.
24. Wenguo, Q.X.; Jin, L.; Zhang, X.Y. Improvement of energy-absorbing structures of a commercial vehicle for crashworthiness using finite element method. *Int J Adv Manuf Technol* **2006**, *30*, 1001 – 1009.

25. Huiwen, H.; Zhenyuan, L.; Wang, J.; Lu, W. Impact crash analyses of an off-road utility vehicle – part I: validation of finite-element model for body structure. *International Journal of Crashworthiness* **2011**, *17*, 153 – 162.
26. Huiwen, H.; Zhenyuan, L.; Wang, J.; Lu, W. Impact crash analyses of an off-road utility vehicle– part II: simulation of frontal pole, pole side, rearbarrier and rollover impact crashes. *International Journal of Crashworthiness* **2012**, *17*, 163 – 172.
27. Moradi, R.; Setpally, R.; Lankarani, H. Use of Finite Element Analysis for the Prediction of Driver Fatality Ratio Based on Vehicle Intrusion Ratio in Head-On Collisions. *Applied Mathematics* **2013**, *4*, 56–63.
28. Zhao, L.; Pawlus, W.; Karimi, H.R.; Robbersmyr, K.G. Data-Based Modeling of Vehicle Crash Using Adaptive Neural-Fuzzy Inference System. *IEEE / ASME Transactions on mechatronics* **2014**, *19*, 684 – 696.
29. Kankariya, N.; F.B.Sayyad. Numerical Simulation of Bumper Impact Analysis and to Improve Design for CrashWorthiness. *International Journal of Engineering and Science (IJES)* **2015**, *4*, 58 – 66.
30. Hickey, A.; Xiao, S. Finite Element Modeling and Simulation of Car Crash. *International Journal of Modern Studies in Mechanical Engineering (IJMSME)* **2017**, *3*, 1 – 5.
31. NHTSA. *Vehicle Crash Test Database*, <http://www-nrd.nhtsa.dot.gov/database/vsr/veh/querytest.aspx>, 2016. Accessed, May 25, 2016.
32. Vetterlil, M.; Kovacevic, J.; Goyal, V.K. *Foundations of Signal Processing*; Cambridge University Press, 2014.
33. Oppenheim, A.V.; Schaffer, R.W.; Buck, J.R. *Discrete-Time Signal Processing*, 2nd ed.; Pentice Hall: New Jersey 07458, 1999.
34. Abramson, M.A. *Algorithm and Direct Search Toolbox User's Guide*; MathWorks, Inc: 3 Apple Hill Driven, 2004.
35. Popov, A.; Sofia, T. *Genetic Algorithms for Optimization-User Manual*, 2003.
36. *LSDYNA Supports*, <https://www.dynasupport.com/howtos/element/hourglass>. Accessed, May 29, 2018.
37. Nasution, R.P.; Siregar, R.A.; Fuad, K.; Adom, A.H. The Effect of ASI (Acceleration Severity Index) to Different Crash Velocities. *Proceedings of International Conference on Applications and Design in Mechanical Engineering (ICADME)*, Batu Ferringhi, Penang, MALAYSIA, 11-13 October, 2009.
38. European Standard EN 1317-2. Road restraint systems Part 2, Performance Classes, impact test acceptance criteria and test method for safety barriers including vehicle parapets. Technical report, European Committee of Standardization, 2010.
39. Shojaat, M. Correlation between injury risk and impact severity index ASI. *Swiss Transport Research Conference, Monte Verità / Ascona, Sweden*, 20 - 22 March, 2003.
40. Gabauer, D.; Hampton, G.C. Comparison of Roadside Crash Injury Metrics using Event Data Recorders. *Accident Analysis and Prevention* **2008**, *40*, 548–558.